PHYSICAL REVIEW B VOLUME 28, NUMBER 8 15 OCTOBER 1983

Green's-function calculation of surface properties associated with adsorption

Y. B. Band
Allied Corporation, 7 Powderhorn Drive, Mount Bethel, New Jersey 07060
and Department of Chemistry, Ben-Gurion University of the Negev, Beer-Sheva 84105, Israel

S. Efrima
Department of Chemistry, Ben-Gurion University of the Negev, Beer-Sheva 84105, Israel
(Received 2 May 1983)

A technique to calculate the single-particle Green's function, and therefore the density of states and other single-particle properties for surface phenomena, is described. The Green's function is constructed from two wave functions, solutions of the Schrödinger equation satisfying boundary conditions in the bulk and in the vacuum. We apply the technique to piecewise constant potential models, where the Green's function can be obtained in analytic form. Results for surface densities of states for these model potentials are presented.

I. INTRODUCTION

The great difficulty of calculating spectra of atoms or molecules adsorbed on surfaces arises because, on one hand, the symmetry of the bulk is broken at the surface, and on the other hand, the atom on the surface is no longer an isolated physical system restricted to a microscopically small region. Consequently, the boundary conditions necessary for such systems are more complicated than those for the bulk or for the isolated atomic entity.

Surface phenomena can be treated in terms of the Green's function (GF) satisfying the appropriate boundary conditions within the bulk and the vacuum. In this paper we present a theoretical framework that is particularly useful for constructing such GF's.

Green's-function methods for treating electronic states in surface problems have been used in the past. Garcia-Moliner and Rubio[1] have suggested a factorization method to obtain the GF at an interface located at the mirror plane between two infinite media. Inglesfield[2] and Velicky and Bartoš[3] generalized the method to more asymmetric cases. Davison *et al.*[4] used this method, with a modification due to Glasser,[5] for the factorization of more complex systems, such as the n-interface problem and virtual surface states. Oxinos and Modinos[6] used this method for studying the electronic structure of atoms adsorbed on metals. This method expresses the surface GF in terms of the GF's and their derivatives for each of the separate media, thus replacing the difficult interface problem with two easier one-phase problems. It is especially convenient for cases of an abrupt potential jump at the interface. Haydock *et al.*[7] calculated the GF in a tight-binding model in the form of an infinite continued fraction. The coefficients are obtained from a basis set localized on each of the atoms. In this method it is difficult to treat cases in which the periodicity of the bulk is modified near the surface or when adsorbed atoms (adatoms) are present. Kalkstein and Soven,[8(a)] using similar methods to those of Allen and Lenghart,[8(b)] treated a semi-infinite solid in the tight-binding limit. They used a Wannier-Bloch mixed representation for the states of the infinite crystal from which they generated the GF for the surface at a cleave plane in the infinite crystal. They also incorporated the effect of alterations in the surface potential. Their method requires dispersion relations of the unperturbed crystal. Restriction of the interactions to nearest neighbors is a great help in the actual application of their method. Lyo and Gomer[9] review some general approaches to the calculation of the GF in its spectral decomposition representation. In these methods, one needs a complete basis set, and, in principle, infinite sums over them [see Eq. (1.7)]. Recently, Kambe[10] described a layer by a GF technique.

In this paper we consider electron surface phenomena treated within the single-particle approximation. That is, we assume that we are given a potential (or pseudopotential) $U(\vec{x})$. Deep inside the bulk the potential is periodic, whereas outside the bulk the potential goes to a constant. At the surface the potential includes the contribution of the adatoms. We shall for simplicity begin by discussing the one-dimensional problem and develop techniques for this case. Generalization to three dimensions is treated only briefly. Other methods of generating integrals over the GF's without directly obtaining the GF are under development but will not be discussed here.

For the potential in Fig. 1 one can ask where are the bound-state energies? What is the density of states (DOS) as a function of energy? What is the DOS in a restricted region of physical space (for instance, that associated with the penetration depth of light)? What is the absorption intensity of light of a given frequency ω_0, $I(\omega_0)$? What is the Raman scattering intensity of incident frequency ω_0 and outgoing frequency ω, $I(\omega_0,\omega)$?

All of these questions can be answered in terms of the GF

$$G_E(Q,Q')=\langle Q \mid (E-H)^{-1} \mid Q' \rangle \ , \tag{1.1}$$

with appropriate boundary conditions, where H is the single-particle Hamiltonian and Q is the position variable. The DOS ρ_E is given by

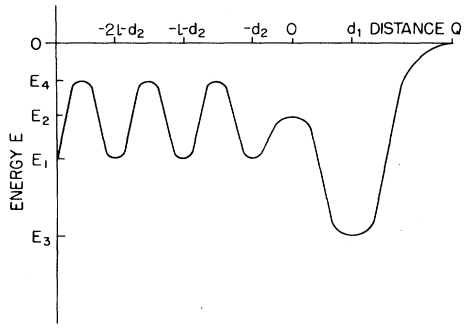

FIG. 1. Schematic representation of an arbitrary one-dimensional potential for an adatom on a solid. l is the bulk periodicity distance.

$$\rho_E = -\pi^{-1}\mathrm{Im}\int_{-\infty}^{\infty} dQ\, G_E(Q,Q) \,. \tag{1.2}$$

The DOS in a restricted region can be defined as

$$\rho_E = -\pi^{-1}\mathrm{Im}\int_{-\infty}^{\infty} dQ\, p(Q) G_E(Q,Q) \,, \tag{1.3}$$

where $p(Q)$ is a function defining this region. For example, for a region defined by the penetration of light with penetration depth λ, one can take

$$p(Q) = \Theta(-Q)\exp(-Q/2\lambda) + \Theta(Q) \,, \tag{1.4}$$

$\Theta(Q)$ being the Heaviside unit-step function. Thus, within the bulk, the penetration factor falls off as the electric field penetration and, outside the bulk, the penetration factor is unity.

The first-order perturbation theory expression for absorption intensity from initial state i at frequency ω_0 is given by

$$\begin{aligned} I_i(\omega_0) &\propto \sum_f |\langle f|X|i\rangle|^2 \delta(\omega_0 + E_i - E_f) \\ &= -\pi^{-1}\mathrm{Im}\int dQ \int dQ' \psi_i^*(Q) X^*(Q) \\ &\quad \times G_{E_f}(Q,Q') X(Q') \psi_i(Q') \,, \end{aligned} \tag{1.5}$$

where $X(Q)$ is the photon-matter interaction Hamiltonian and $\psi_i(Q)$ is the wave function of the initial state.

The lowest- (second-) order contribution to the Raman spectrum from an initial state i to a final state f, with incident-photon frequency ω_0 is as follows:

$$\begin{aligned} I_i(\omega_0,\omega) &\propto \int dQ \int dQ' \psi_f^*(Q) X(Q) \\ &\quad \times G_{E_i+\omega}(Q,Q') X(Q') \psi_i(Q') \end{aligned} \tag{1.6}$$

(actually this is the resonance contribution of the Raman transition amplitude). In fact, any single-particle observable can be calculated in the form of a double integral

$$\int dQ \int dQ' \alpha(Q) G(Q,Q') \beta(Q') \,,$$

with weighting functions $\alpha(Q)$ and $\beta(Q')$.

Bound states are also obtained from the GF. Bound-state energies occur where the GF has poles, or the Wronskian has roots. Consequently, knowledge of the GF with the correct boundary conditions is a prerequisite to providing the answer to the questions raised above.

One can now ask, what are the correct boundary conditions to impose on the GF? To answer this question one must consider the physics of the process under consideration. For the calculation of bound states, DOS, and absorption or Raman scattering, we can divide the energy regime into four regions. For energies below E_1, in Fig. 1 the GF $G_E(Q,Q')$ must decay as $Q \to \pm\infty$ (true bound states). For energies above E_1 but below E_4, it must decay as $Q \to \infty$, and as $Q \to -\infty$ it must be periodic, if the potential $U(Q)$ is real; but, if $U(Q)$ contains an absorptive part, then $G_E(Q,Q')$ must also decay as $Q \to -\infty$. For energies above E_4 but below zero, the GF should behave essentially like outgoing waves as $Q \to -\infty$, and must decay as $Q \to \infty$. Only when $E > 0$ does one obtain outgoing waves as $Q \to \pm\infty$.

One way to express the GF $G_E(Q,Q')$ is in terms of its spectral representation[9]

$$G_E(Q,Q') = \sum_i \frac{\psi_{\epsilon_i}(Q)\Psi_{\epsilon_i}^*(Q')}{E - \epsilon_i} \,. \tag{1.7}$$

Since all the energy eigenvalues ϵ_i lying above E_1 of Fig. 1 must be included in the above sum (integral), the boundary conditions on the wave functions $\Psi_{\epsilon_i}(Q)$ and $\psi_{\epsilon_i}(Q)$ for ϵ_i in the continuous spectrum are important in the construction of G_E with the correct boundary conditions. In fact, the spectral decomposition of G_E in Eq. (1.6) is not of any great practical value unless the sum over i is truncated to a finite discrete sum of states. But in this case it will be difficult to accurately ascertain G_E for E in the continuous spectrum.

In this paper we present an alternative method of constructing the one-particle GF. G_E is constructed from the wave functions $s(Q)$ and $h(Q)$, which are solutions of the Schrödinger equation at energy E, satisfying a boundary condition on the left-hand side and right-hand side, respectively.[11] The necessity of calculating sums over energy eigenvalues required in Eq. (1.7) is alleviated.

In Sec. II we outline the calculation of G_E for the arbitrary one-dimensional potential of Fig. 2. In Secs. III and IV we present and explain the results of the local surface DOS for the potentials of Figs. 2 and 3, respectively. (Our choice of discussing the local DOS, rather than some excitation function, which is weighted with some appropriate surface weighting factor, is arbitrary.) These model calcu-

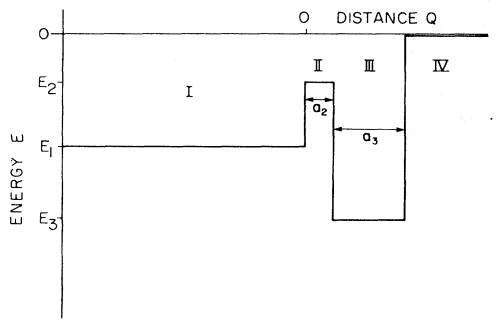

FIG. 2. Potential vs position—uniform solid.

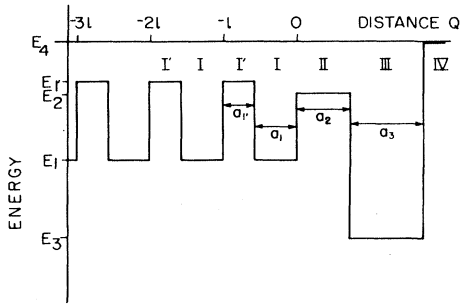

FIG. 3. Potential vs position—periodic solid.

lations can be carried through, almost analytically, using the present method. They illustrate the implementation of the method. Section IV contains the generalization of this method to three dimensions.

II. CONSTRUCTION OF $G_E(Q,Q')$

We wish to construct the GF for a single particle in the potential shown in Fig. 1 for an arbitrary energy E. Consider, for simplicity, an energy E below the asymptotic value of the potential on the right-hand side, but above the minimum of the potential inside the bulk on the left-hand side. Physically, it is clear that we require the boundary conditions

$$\begin{aligned} &G_E(Q,Q')\sim\exp\{-[2\mu\,|\,E-U(Q)\,|\,]^{1/2}Q\}\ , \quad Q\to\infty \\ &G_E(Q,Q')\sim\text{Bloch wave}\ , \quad Q\to-\infty\ . \end{aligned} \tag{2.1}$$

Now, for an arbitrary potential, the GF satisfying two-point boundary conditions at Q_a and Q_b with $Q_a<Q_b$ is given by[11]

$$\begin{aligned} G_E(Q,Q')=2\mu W^{-1}[&s(Q)h(Q')\Theta(Q'-Q) \\ &+h(Q)s(Q')\Theta(Q-Q')]\ , \end{aligned} \tag{2.2}$$

where μ is the particle mass, Θ is the Heaviside unit-step function and s and h are solutions to the Schrödinger equation at energy E. $s(Q)$ satisfies the boundary condition at Q_a and $h(Q)$ satisfies the boundary condition at Q_b. W is the Wronskian of s and h, viz.,

$$W=s(Q)h'(Q)-s'(Q)h(Q)\ , \tag{2.3}$$

where W is a constant, i.e., independent of Q, as can readily be shown by differentiating W and using the Schrödinger equation for s and h. $G_E(Q,Q')$ then satisfies both of the boundary conditions, and is a solution of the equation

$$[E-H(Q)]G_E(Q,Q')=\delta(Q-Q')\ , \tag{2.4}$$

where δ is the Dirac function.

In our case, Q_b is in the vacuum region, and asymptotically the wave function

$$h(Q)\sim\exp(i\{2\mu[E-U(Q)]\}^{1/2}Q)\ , \quad Q\to\infty\ . \tag{2.5}$$

Q_a is deep in the interior of the bulk. Thus the wave function $s(Q)$ is a periodic wave function inside the bulk, if E is within a band, and will in general diverge as $Q\to\infty$. If E is within a band gap, then $s(Q)$ should decrease as $Q\to-\infty$ in the sense that

$$s(Q+l)=\lambda S(Q)\ , \quad |\lambda|>1\ . \tag{2.6}$$

Here Q is in the bulk and l is the periodicity of the solid. For an arbitrary energy E within a band there are two periodic solutions. We seek the solution which decays as one moves further into the bulk from the surface, if a small absorptive part is added to the potential, $U(Q)\to U(Q)-i\omega$, $\omega>0$. That is, the wave function satisfies Eq. (2.6) for $\omega>0$.

The solution $h(Q)$ can be easily obtained by integrating the Schrödinger equation from outside the bulk into the bulk, beginning the solution at two adjacent values of Q as the exponential function in Eq. (2.5).

The wave function $s(Q)$ can be constructed in the following manner. At a given point well inside the bulk where $V(Q)$ is minimum, for instance, Q_0, we can construct two linearly independent wave functions $\psi_1(Q)$ and $\psi_2(Q)$, such that

$$\psi_1(Q_0)=1\ , \quad \psi_1'(Q_0)=0 \tag{2.7}$$

and

$$\psi_2(Q_0)=0\ , \quad \psi_2'(Q_0)=1\ . \tag{2.8}$$

With these initial conditions at Q_0, we integrate $\psi_1(Q)$ and $\psi_2(Q)$ over one period in the bulk to the point Q_0+l. We construct $s(Q)$ as a linear combination of ψ_1 and ψ_2,

$$s(Q)=\beta\left[\frac{\alpha}{\beta}\psi_1(Q)+\psi_2(Q)\right]\ , \tag{2.9}$$

where α and β are chosen so that

$$s(Q+l)=\lambda s(Q)\ , \tag{2.10}$$

$$s'(Q+l)=\lambda s'(Q)\ . \tag{2.11}$$

These equations, evaluated at $Q=Q_0$, yield two equations for α/β and λ which can be solved simultaneously to give

$$\alpha/\beta=\frac{\psi_2(Q_0+l)}{\lambda-\psi_1(Q_0+l)}\ , \tag{2.12}$$

$$\begin{aligned} \lambda_\pm=&\frac{\psi_1(Q_0+l)+\psi_2'(Q_0+l)}{2} \\ &\pm\left[\left[\frac{\psi_1(Q_0+l)+\psi_2'(Q_0+l)}{2}\right]^2-1\right]^{1/2}\ . \end{aligned} \tag{2.13}$$

In obtaining (2.13) we have used the fact that the Wronskian of ψ_1 and ψ_2 equals unity.

One can now determine which of the roots λ in Eq. (2.13) is greater than unity in magnitude for small ω. A useful relationship is

$$\lambda_+=1/\lambda_-\ . \tag{2.14}$$

Taking the limit $\omega\to0$, enables us to determine the correct root at the energy E. Substituting λ into Eq. (2.12), setting $\beta=1$ (an arbitrary choice of a multiplication factor, which does not affect the GF), and using Eq. (2.9), gives the solution $s(Q)$ over the region $Q_0\le Q\le Q_0+l$.

To obtain $s(Q)$ over other regions, where the potential is periodic (i.e., inside the bulk), Eq. (2.10) is merely used repeatedly; $s(Q+2l)=\lambda^2 s(Q)$, etc. When we approach the surface, the potential looses the periodicity of the bulk. We can then begin integrating the Schrödinger equation through the surface region into the vacuum. Having found $s(Q)$ and $h(Q)$, we substitute them into Eq. (2.2) and the required GF with the appropriate boundary conditions is obtained.

We shall now discuss applications to the model potentials in Figs. 2 and 3, in order to gain some physical insight into the nature of the simplest surface problems.

III. ADATOM ON A SEMI-INFINITE SOLID

In order to become familiar with the above method of constructing the GF and with the dependence of surface DOS's upon the width and depth of the atomic potential, the distance of the adatom from the surface and the depth of the bulk potential, we consider the potential shown in Fig. 2.

The wave function in the region j (= I, II, III, IV) at any given energy E may be written as

$$f_{j,p}(Q)=A_{j,p}e^{ik_jQ}+B_{j,p}e^{-ik_jQ}\ ,\quad P=s,h \tag{3.1}$$

where $f_{j,p}(Q)=s_j(Q)$ or $h_j(Q)$, for $p=s$ or h, respectively. The momentum in region j is

$$k_j=[2\mu(E-U_j)]^{1/2}\ , \tag{3.2}$$

which can be either real or pure imaginary (for U_j real).

The boundary conditions determine some of the coefficients A_j and B_j. Matching the wave function and its derivative at the boundary regions determines the others. We require

$$s(Q)\to e^{-ik_1Q}\ \text{ as } Q\to-\infty \tag{3.3}$$

where the proportionality constant is unimportant and is taken as unity.

An easy wasy to see the validity of Eq. (3.3) is by considering energies E such that $E<V_1$. Then $k_1=i\,|k_1|$ and

$$s(Q)\to e^{|k_1|Q}\to 0\ \text{ as } Q\to-\infty \tag{3.4}$$

as it should.

Similarly, one requires

$$h(Q)\to e^{ik_4Q}\ \text{ as } Q\to\infty \tag{3.5}$$

thus satisfying the boundary condition on the right-hand side.

These conditions result in the following relationships:

$$A_{1,s}=0\ ,\quad B_{1,s}=1 \tag{3.6}$$
$$A_{4,h}=1\ ,\quad B_{4,h}=0\ .$$

The A,B coefficients in the other three regions are obtained using the transformation

$$\underline{A}_{j+1,p}=(\underline{T})_{j+1,j}\underline{A}_{j,p}\ , \tag{3.7}$$

where

$$\underline{A}_{j,p}=\begin{bmatrix}A_{j,p}\\ B_{j,p}\end{bmatrix}\ , \tag{3.8}$$

and

$$(\underline{T})_{j+1,j}=\frac{1}{2k_{j+1}}\begin{bmatrix}(k_j+k_{j+1})e^{i(k_j-k_{j+1})l_j} & (k_{j+1}-k_j)e^{-i(k_j+k_{j+1})l_j}\\ (k_{j+1}-k_j)e^{i(k_j+k_{j+1})l_j} & (k_{j+1}+k_j)e^{-i(k_j-k_{j+1})l_j}\end{bmatrix}\ , \tag{3.9}$$

which arise from matching the wave functions and their derivatives across the boundaries of the regions. In Eq. (3.9), l_j is the coordinate of the boundary between region j and $j+1$.

The Wronskian in any region j, is given by

$$W(s,h)=2ik_j(B_{j,s}A_{j,h}-B_{j,h}A_{j,s})\ . \tag{3.10}$$

In region I or IV, one obtains a particularly convenient form

$$W(s,h)=2ik_1A_{1,h}=2ik_4B_{4,s}\ . \tag{3.11}$$

It is now easy to calculate the DOS and any local DOS using Eq. (1.3) and the GF for this case.

For demonstration purposes we calculate the local DOS in each of the four regions taking the function $p(Q)$ of Eq. (1.3) to be of the simple form

$$p_j(Q)=\begin{cases}1 & \text{in region } j\\ 0 & \text{outside region } j\ .\end{cases} \tag{3.12}$$

Equations (3.14)—(3.17) give the results for the quantities G_j, which are the integrals of the diagonal GF, $G_E(Q,Q)$ in the region j. The DOS in that region is given by

$$\rho_j(E)=-\pi^{-1}\mathrm{Im}\bar{G}_j\ , \tag{3.13}$$

where $\bar{G}_j=\int dQ\,p_j(Q)G(Q,Q)$. In region I, we obtain

$$\bar{G}_{\mathrm{I}}=\frac{a_1}{2ik_1}+\frac{W^{-1}B_{1,h}}{2ik_1}(e^{2ik_1a_1}-1)\ . \tag{3.14}$$

In region IV, we find

$$\bar{G}_{\mathrm{IV}}=\frac{a_4}{2ik_4}+\frac{W^{-1}A_{4,s}}{2ik_4}e^{2ik_4(a_3+a_2)}(e^{2ik_4a_4}-1)\ , \tag{3.15}$$

a_1 and a_4 being the lengths of the domains probed in regions I and IV, respectively.

$\bar{G}$ in regions II and III is given by

$$\begin{aligned}\bar{G}_{\mathrm{II}}=W^{-1}[&(B_{2,s}A_{2,h}+B_{2,h}A_{2,s})a_2\\ &+A_{2,s}A_{2,h}(e^{2ik_2a_2}-1)/2ik_2\\ &-B_{2,s}B_{2,h}(e^{-2ik_2a_2}-1)/2ik_2]\ ,\end{aligned} \tag{3.16}$$

$$\bar{G}_{\mathrm{III}}=W^{-1}[(B_{3,s}A_{3,h}+B_{3,h}A_{3,s})a_3 + A_{3,s}A_{3,h}(e^{2ik_3a_3}-1)e^{2ik_3a_2}/2ik_3 - B_{3,s}B_{3,h}(e^{-2ik_3a_3}-1)e^{-2ik_3a_2}/2ik_3] \ . \quad (3.17)$$

The main contribution for energies $E > U_1$ to the DOS in region I is

$$\rho_1(E) \propto \frac{a_1}{2k_1} \ , \quad (3.18)$$

which leads to the well-known one-dimensional DOS per unit length of a particle in a box, $1/k_1$. The factor $\frac{1}{2}$ in Eq. (3.18) stems from the semi-infinite nature of the solid we consider here. The second term on the right-hand side of Eq. (3.14) for the DOS in region I is due to the presence of the surface. Its contribution is clearly negligible for large a_1.

In region IV there is no bulklike DOS for $E < U_4$, since k_4 is a pure imaginary. However, the surface term in (3.15) manifests itself by decaying away from the surface.

We present below the results of our calculation of the DOS in region III for the full potential as shown in Fig. 2. We chose, as a standard case, a set of parameters which sustains two bound states in the isolated atomic potential well. One is a deep state, which is below the level of the (uniform) metal potential well. It therefore remains bound also in the adsorbed configuration. The second bound state is degenerate in energy to levels in the solid. The standard parameters are $U_1=-20$ eV, $U_2=0$ eV, $U_3=-30$ eV, $U_4=0$ eV, $a_2=2$ bohr, and $a_3=3$ bohr.

The calculation itself is divided into three separate parts. First we calculate the (bound) states of the isolated atom, i.e., for a potential of the form $U_1=U_2=U_4=0$ and $U_3\neq 0$.[12] The second and third phases of the calculation pertain to the adatom situation, as shown in Fig. 2. We compute the bound-state energies by searching for the roots of the Wronskian function. Then we calculate the DOS in the energy region above U_1. All energy units are given in eV and DOS in units of eV^{-1}.

In Fig. 4 we show the bound-state energies and the DOS as a function of energy in region III. The solid line indicates the DOS, whereas the dashed line indicates its logarithm. The position of the isolated-atom energy level is also marked.

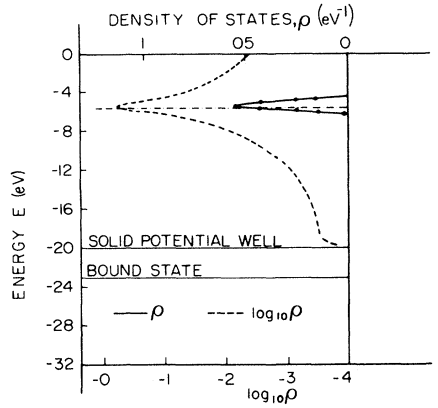

FIG. 4. Density of states in region III and its logarithm—standard case: $U_1=-20$ eV, $U_2=0$ eV, $U_3=-30$ eV, $U_4=0$ eV, $a_2=2$ bohr, and $a_3=3$ bohr. Solid line shows DOS. Dashed line shows logarithm of DOS.

The atomic state which remains bound even when the atom is adsorbed on the surface is only slightly modified by the interaction with the surface. It is slightly stabilized as expected by about 0.009 eV (its energy is 23.1 eV). The stabilization energy peaks dramatically when the depth of the metal potential energy is near the isolated atom energy (Table I). For example, when U_1 is changed to -22 eV from -20 eV, and all other parameters are left constant, the stabilization grows to 0.012 eV.

Upon adsorption the higher-energy state of the atomic well turns into a resonance, with full width at half maximum (FWHM) of about 0.4 eV (lifetime of about 10^{-14} sec), the line shape is asymmetric with a slower decreasing tail on the high-energy side. This is understood in light of the growing tunneling probability with increasing energy.

The center of the resonance state is shifted in energy as compared to the isolated atomic state. Interestingly, the shift is toward higher energies (destabilization). In the standard case this shift is 0.15 eV.

Perturbation theory would predict downward shifts proportional to U_1 and the tunneling probability. However, the repulsion between the atomic level and the "metal" levels works in opposition to this expectation, at least in

TABLE I. State shifts and widths—uniform metal. $U_3=-20$ eV, $U_2=U_4=0$ eV, $a_2=2$ bohr, and $a_3=3$ bohr. E_c is the "center of mass" of solid levels (see text). E is the position of levels. Δ is the shift of the levels as compared to an isolated atom. $\delta\uparrow$ and $\delta\downarrow$ are the high- and low-energy widths of the resonative states. U_1 is position of solid potential well.

		Resonance state				Bound state			
U_1 (eV)	E_c (eV)	E (eV)	Δ (eV)	$\delta\downarrow$ (eV)	$\delta\uparrow$ (eV)	E (eV)	Δ (eV)	$\delta\downarrow$ (eV)	$\delta\uparrow$ (eV)
−40	−26.7	−5.296	0.267	0.284	0.296	−23.108	−0.003	0.019	0.019
−30	−20.0	−5.340	0.223	0.315	0.330	−23.116	−0.010	0.015	0.015
−22	−14.7	−5.395	0.168	0.345	0.461	−23.117	−0.012		
−20	−13.3	−5.415	0.148	0.355	0.464	−23.114	−0.009		
−10	−6.7	−5.637	−0.074	0.353	0.482	−23.108	−0.003		
−6	−4.0	−5.893	−0.330	0.067	0.537	−23.107	−0.002		
−5.95	−3.97	−5.896	−0.333	0.043	0.113	−23.107	−0.002		
−5.90	−3.94	−5.896	−0.333	0.004	0.025	−23.107	−0.002		

the standard case. This can be rationalized if one replaced the metal levels by one level placed at their "center of energy" E_c. For the uniform (flat) solid

$$E_c = 2U_1/3 \ . \tag{3.19}$$

Thus, roughly, only (isolated) atomic levels which are higher in energy than E_c will be shifted upwards, while atomic levels more stable than E_c will be further stabilized on the surface.

This prediction should hold as long as the interaction with the metal levels is not strong (i.e., for high and wide barriers in region II). For state energies near E_c, these predictions will not hold, because interactions with higher-energy metal levels are stronger than with lower-energy levels.

Figure 5 shows the dependence of the position of the resonance state and its width on the depth of the metal potential-energy well U_1. All the parameters are those of the standard case, except U_1 which varies between -40 and -5.90 eV. The main results are summarized in Table I.

Table I also shows how the widths change. The DOS is limited below by U_1. On the high-energy less stable side, no such restrictions occur. Indeed, in Fig. 6 we see that the energy-level density extends smoothly into the continuum.

The nature of the discontinuity in the surface DOS is interesting. We find that a power-law behavior in the energy above threshold does not fit the cutoff of the DOS near U_1.

In Fig. 6, we plot the DOS as a function of a_2, the distance of the atom from the surface. All other parameters are those of the standard case. The cutoff of the surface DOS at U_1 is especially noticeable for small a_2. For these small values of a_2, the bound-state energy is significantly affected as well.

The widths of the resonance state are exponentially dependent on a_2. In Fig. 7 we plot log δ (δ is half of the FWHM) as a function of a_2 and compare it with the function

$$\log\left[\exp\left[-2\int_0^{a_2} dQ[2\mu(U_2-E)]^{1/2}\right]\right] .$$

This function is proportional to the tunneling probability through the barrier of region II at energy E. The energy

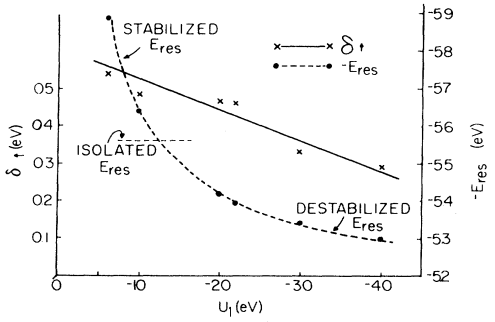

FIG. 5. Resonance energy shift (dashed line) and high-energy width δ_4 (solid line and $\times$) vs U_1 for uniform solid.

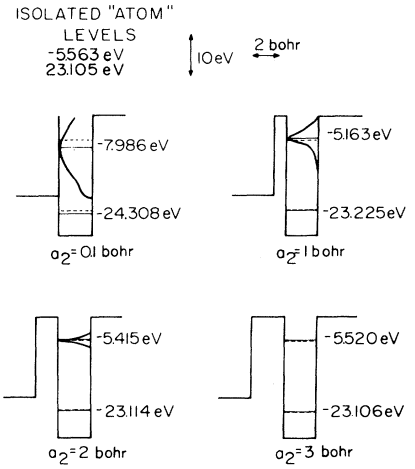

FIG. 6. Bound states and DOS in the atomic well (region III) for uniform solid. Densities are normalized in each case to their maximum value. Potential parameters are $U_1=-20$ eV, $U_2=U_4=0$ eV, $U_3=-30$ eV, $a_3=3$ bohr, and $a_2=0.1,1,2,$ and 3 bohr.

is taken as that of the resonance state. The slope of the two plots differ by less than 4%. Figure 8 summarizes the dependence of the system behavior on U_2, the height of the barrier.

In this section we applied the direct GF formalism to a simple, flat potential-energy (one-dimensional) metal model. We computed the density of bulk and surface states and discussed their dependence on various system parameters.

IV. ADATOM ON SEMIFINITE KRONIG-PENNEY SOLID

We turn now to the model potential shown in Fig. 3 to illustrate the technique for treating a periodic bulk poten-

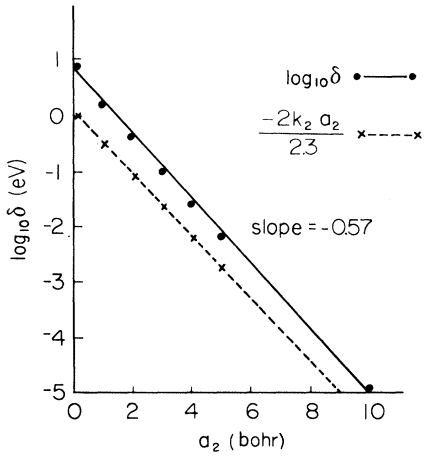

FIG. 7. Logarithm of the level half-width δ vs a_2 (solid line) and tunneling probability vs a_2 (dashed line) for uniform solid. Potential parameters are $a_3=3$ bohr, $U_1=-20$ eV, $U_2=U_4=0$ eV, and $U_3=-30$) eV.

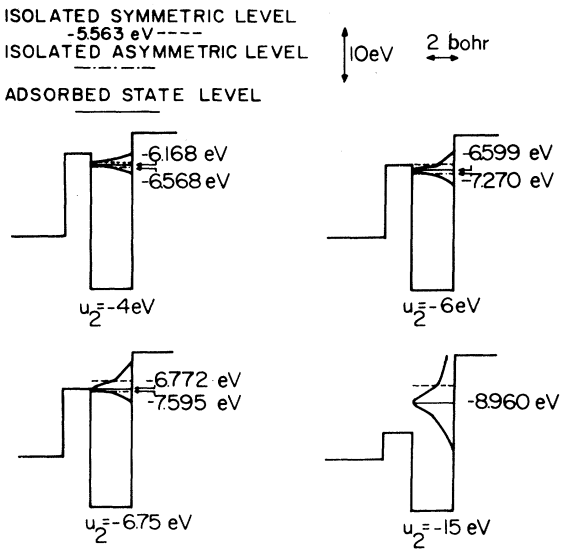

FIG. 8. DOS in the atomic well (region III) for different U_2 values for uniform solid. Densities are normalized in each case to their maximum value. Potential parameters are $U_1=-20$ eV, $U_3=-30$ eV, $U_4=0$ eV, $a_2=2$ bohr, $a_3=3$ bohr, and $U_2=-4$, -6, -6.75, -15 eV.

tial. The wave function $h_E(Q)$ for $Q\in(\infty,0]$ is identical to the previous model potential. The wave function $s_E(Q)$ must be periodic when E lies within a band, whereas it decreases as one recedes into the bulk when E is within a band gap. In order to treat all energies in the same fashion in constructing the wave function $s(Q)$, it is convenient to add an arbitrary small absorptive part to the bulk potential $U(Q)\rightarrow U(Q)-i\omega$.

As discussed in Sec. II, we construct the two linearly independent solutions $\psi_1(Q)$ and $\psi_2(Q)$ of Eqs. (2.7) and (2.8). For simplicity we choose $Q_0=-3l$, where $l=a_1+a_{1'}$. Owing to the simple form of the potential, the integrations yielding ψ_1 and ψ_2 may be performed analytically. The wave function satisfying (2.7) is then given by

$$\psi_1(Q)=\cos[k_{1'}(Q-Q_0)]\ ,\ k_{1'}=\{2\mu[E-(U_{I'}-i\omega)]\}^{1/2}\ , \tag{4.1}$$

in region I' between $(-3l,2l-a_1)$, while for $(-2l-a_1,-2l)$ we have

$$\psi_1(Q)=A_1e^{ik_1Q}+B_1e^{-ik_1Q}\ ,\ k_1=\{2\mu[E-(U_I-i\omega)]\}^{1/2}\ . \tag{4.2}$$

The wave function ψ_1 and its derivative ψ_1' are continuous across $Q=-2l-a_1$. These two conditions are sufficient to determine (A_1,B_1). Similarly,

$$\psi_2(Q)=\begin{cases} k_{1'}^{-1}\sin[k_{1'}(Q-Q_0)]\ , & -3l\le Q\le -2l-a_1 \\ A_2e^{ik_1Q}+B_2e^{-ik_1Q}\ , & -2l-a_1\le Q\le -2l \end{cases} \tag{4.3}$$

and (A_2,B_2) are determined by continuity of ψ_1 and ψ_1' across $Q=2l-a_1$. Since $\psi_1(Q_0+l)$ and $\psi_2(Q_0+l)$, where $Q_0+l=-2l$, are easily determined, the roots λ of Eq. (2.13) may be obtained. We choose the root whose magnitude is greater than unity (for infinitesimal ω), substitute into Eq. (2.12) to obtain α/β and then form $s(Q)$ from Eq. (2.9).

To obtain $s(Q)$ in region II we need to know the values of $s(Q)$ and $s'(Q)$ at $Q=0$ which are easily found using Eqs. (2.10) and (2.11). In region II, $s(Q)$ can be written as in Eq. (3.1), where $(A_{2,s},B_{2,s})$ are obtained from the continuity of $s(Q)$ and $s'(Q)$ across $Q=0$. A similar procedure is employed to go from II to III and then from, III to IV. Now we have $s_E(Q)$ and $h_E(Q)$ in all the regions and the GF is easily formed. The DOS in each of the regions can be obtained from the expressions given in Eqs. (3.13)—(3.17), where the Wronskian is given by Eq. (3.10).

In this section we describe the effect of the bands and band gaps of the solid on the bound states and the DOS of region III, the "adatom" potential-well region. We first compute the bulk DOS of the solid in order to locate the bands and their edges. Our model potential for the solid is the Kronig-Penney potential.[13] The secular equation for the Kronig-Penney potential is given by

$$[(L^2-K^2)/2LK]\sinh(La_{1'})\sin(Ka_1)+\cosh(La_{1'})\cos(Ka_1)=\cos[k(a_1+a_{1'})]\ , \tag{4.4}$$

where

$$L^2=2\mu(U_{1'}-E)\ ,\qquad K^2=2\mu(E-U_1)\ . \tag{4.5}$$

Energies such that the left-hand side of Eq. (4.4) is outside of $(-1,1)$ are in the band gap, all other energies are within the bands.

The DOS in the solid is given by

$$\rho(E)=\rho(k)(dE/dk)^{-1}\ , \tag{4.6}$$

where $\rho(k)=2$, and dE/dk can be extracted from the differentiation of Eq. (4.4) with respect to k,

$$\frac{dE}{dk}=-\frac{(a_1+a_{1'})}{\mu}\sin[k(a_1+a_{1'})]\left[\frac{-(L^2+K^2)^2}{2(LK)^3}\sinh(La_{1'})\sin(Ka_1)+\left[\frac{L^2-K^2}{2LK}\frac{a_1}{K}-\frac{a_{1'}}{L}\right]\sinh(La_{1'})\cos(Ka_1)-\left[\frac{L^2-K^2}{2LK}\frac{a_{1'}}{L}+\frac{a_{1'}}{K}\right]\cosh(La_{1'}\sin(Ka_1)\right]\ . \tag{4.7}$$

With the use of Eqs. (4.6) and (4.7), and the dispersion relation $k(E)$ from Eq. (4.4) the DOS in the bulk metal can be obtained.

We can now easily calculate both the metal bulk DOS and the DOS at the position of the adatom. In the following figures we show the results of such calculations.

Throughout these calculations we took $U_2=U_4=0$ eV, $U_3=-30$ eV, $U_1=-20$ eV, $a_2=2$ bohr, $a_3=3$ bohr, $a_{1'}=4$ bohr, and allowed a_1 and U_1 to vary. U_3 and a_3 were chosen, as in the standard case of Sec. III, to support two states. One bound state remains bound and the other turns into a resonance. a_2 was chosen to facilitate significant interaction (tunneling) between the metal and adatom. Figure 9 shows the DOS in region III, for $U_{1'}=-10$ eV and $a_1=20$ bohr. ρ is plotted on a logarithmic scale to encompass the whole range of energies (-20 eV,0). The positions of the bands of the solid are indicated in Fig. 9. One sees that the atomic state becomes a resonance within the band energy region. The shape of the resonance is quite asymmetric. The peak of the resonance is shifted to -5.50 eV from the position of the isolated atomic state (at -5.56 eV). The FWHM of the resonance is 0.41 eV, compared to 0.8 eV for the resonance interacting with the uniformly flat potential solid, which indicates reduced interaction in this case. Note, in Fig. 9, the tunneling of the bulk DOS into region III. The contribution of the bulk states is rather small. However, it is still noticeable, even for the relatively high and wide barrier used here. For comparison, the DOS of the bulk itself is shown in Fig. 10.

It is interesting to note that when the bulk states penetrate the barrier of region II and "spill over" into region III, the bands change their shape. Higher energies in the band have higher tunneling probabilities. Consequently, the bands are skewed towards the high-energy side. Only near the resonance state does this picture change.

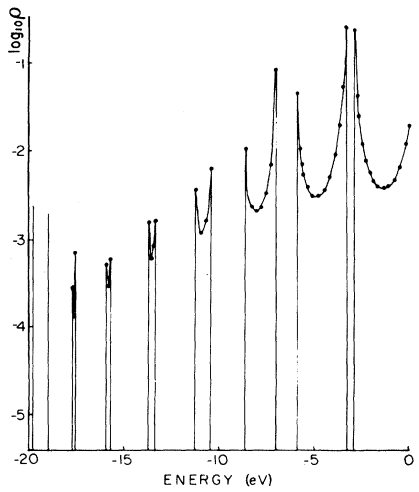

FIG. 10. Logarithm of DOS vs energy. Potential parameters are $U_1=-20$ eV, $U_1=-10$ eV, $a_1=20$ a.u., and $a_{1'}=4$ a.u. Heights of the sharp bands as shown here are not significant, only their positions.

Similar effects were discussed by Kalkstein and Soven[7] and by Haydock *et al.*[6]

In Fig. 11 we show the effect of increasing the barriers inside the metal, i.e., $U_{1'}=-5$ eV. The dashed lines in Fig. 11 show the positions and widths of the bulk bands. A significant narrowing of the bands occur, as compared to the previous calculation. A striking feature of this fig-

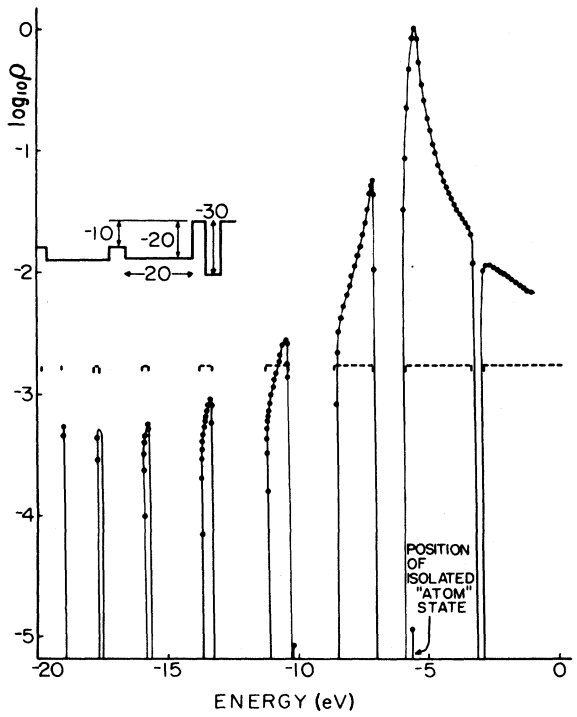

FIG. 9. Logarithm of DOS in region III. Potential parameters are $U_1=-20$ eV, $U_1'=-10$ eV, $U_2=U_4=0$, $U_3=-30$ eV, a_1-20 bohr, $a_1'=4$ bohr, $a_2=2$ bohr, and $a_3=3$ bohr. Dashed lines show positions of bulk solid bands.

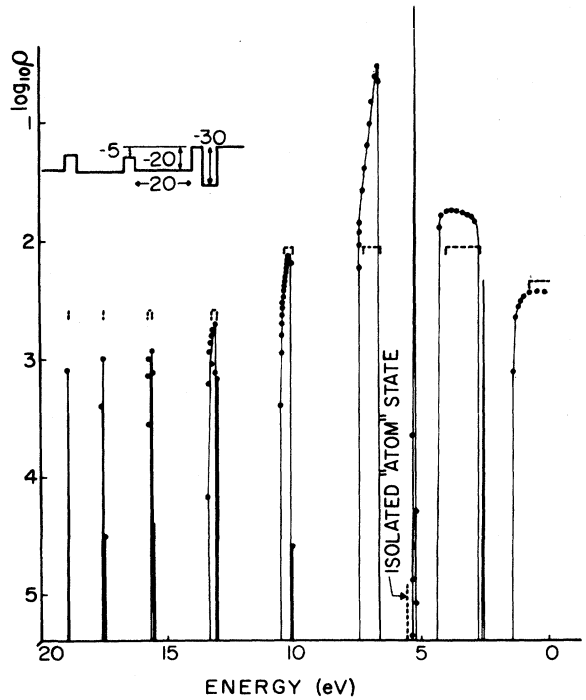

FIG. 11. Logarithm of DOS in region III. Dashed lines show position of bulk bands. Potential parameters are $U_1=-20$ eV, $U_1=-5$ eV, $U_2=U_4=0$, $U_3=-30$ eV, $a_1=20$ bohr, $a_1=4$ bohr, $a_2=2$ bohr, and $a_3=3$ bohr. Height of sharp structures are not significant, only their positions.

ure is that when the bound state is within a band gap it remains almost bound. The width of the resonance state formed is very small. Its width, in this case, is smaller than 0.0002 eV (the resolution of our calculation). We find the density to change from 40 eV^{-1} at $E=5.2612$ eV to 0.2 eV^{-1} at $E=5.2610$ eV. The shift from the bound atomic state is 0.3 eV to higher energies. This can be compared to a shift of 0.15 eV for the flat bulk potential model and 0.06 eV for a periodic metal model with $U_1=-10$ eV. Another feature in Fig. 11 is the broadening of the high-energy bands of the solid, which manage to penetrate the barrier. Also evident are some very sharp structures near the higher-energy side of most of the bands. These sharp states are not present in the DOS of the pure bulk. We attribute them to surface states pulled out of the bulk. These surface states penetrate region II under the barrier in region II. In fact, these states appear regardless of the nature of the potential in region III (e.g., they are still present when $U_3=U_4=0$). They originate from the solid, as can easily be seen by their dependence on the width of the barrier a_2.

V. THREE-DIMENSIONAL GENERALIZATION

In the preceding sections, we detailed the construction of the GF $G_E(Q,Q')$ with the appropriate boundary conditions for one-dimensional surface problems. We explicitly constructed the GF for the potentials of Figs. 2 and 3, and presented results of calculations for the local surface DOS and bound states of these potentials. Clearly, once $G_E(Q,Q')$ is formed, we can form $I_i(\omega)$, $I_i(\omega_0,\omega)$, etc. All single-particle properties can be obtained from the GF.

We now turn to the three-dimensional generalization of the one-dimensional results. We consider a one-particle potential (or pseudopotential) $U(\vec{x})$, which is periodic parallel to the surface directions perpendicular to the normal of the surface ($\hat{z}$ direction). The bulk periodicity inside the material is broken at the surface. A wave function $\Psi(\vec{x})$ in the surface region can be written using the Laue representation in which the Fourier expansion in the parallel coordinates is combined with the coordinate representation in the normal direction.[14]

$$\Psi_{\vec{k}_{||}}(\vec{x})=\sum_{\vec{g}_{||}}^{N}\psi_{\vec{g}_{||}}(z)e^{i(\vec{k}_{||}-\vec{g}_{||})\cdot\vec{x}} , \tag{5.1}$$

where the number of $\vec{g}_{||}$ components retained in the sum is denoted by N and where $\vec{k}_{||}$ is the component of the momentum parallel to the surface. The Schrödinger equation for $\Psi_{\vec{k}_{||}}(\vec{x})$ at energy E then becomes[15]

$$\left[E-\left[-(2\mu)^{-1}\frac{d^2}{dz^2}+\frac{|\vec{k}_{||}-\vec{g}_{||}|^2}{2\mu}+U_0(z)\right]\right]\psi_{\vec{g}_{||}}(z) =\sum_{\vec{g}'_{||}}U_{\vec{g}_{||}-\vec{g}'_{||}}(z)\psi_{\vec{g}'_{||}}(z) . \tag{5.2}$$

These equations can be written in matrix form

$$[E\underline{\mathbb{1}}-\underline{\mathscr{H}}(z)]\underline{\Psi}(z)=\underline{0} , \tag{5.3}$$

where the rows and columns of the matrices are labeled by the N normal momentum vectors. This is a multichannel Schrödinger equation in which each column is an equation of the form (5.2) where the incident term is labeled by the column vector $\vec{g}_{||}$.

It can be shown[16,17] that the GF $\underline{G}(z,z')$, of the equation

$$[E\underline{\mathbb{1}}-\underline{\mathscr{H}}(z)]\underline{G}(z,z')=\delta(z-z')\underline{\mathbb{1}} , \tag{5.4}$$

satisfying two-point boundary conditions, can be written in terms of the solutions $\underline{S}(z)$ and $\underline{H}(z)$ of the Schrödinger equation (5.3) with these boundary conditions, i.e.,

$$\underline{G}(z,z')=2\mu[\underline{S}(z)(\underline{W}^{+})^{-1}\underline{H}(z)\Theta(z-z') +\underline{H}(z)\underline{W}^{-1}\underline{S}^{+}(z')\Theta(z-z')] , \tag{5.5}$$

where the Wronskian matrix $\underline{W}$ given by

$$\underline{W}(\underline{S},\underline{H})=S^{+}(z)\underline{H}'(z)-\underline{S}^{+'}(z)\underline{H}(z) ,$$

is a constant matrix (as can be demonstrated using the Schrödinger equation). The symbol + indicates transpose for the type of boundary conditions we need here. In the present case, $\underline{S}(z)$ is such that, within the bulk,

$$\underline{S}(z+l)=\lambda\underline{S}(z)$$

and

$$\underline{H}(z)\sim\exp i\sqrt{2\mu[E\underline{\mathbb{1}}-\underline{U}(z)]}\ \text{ as } z\to\infty .$$

Thus the multichannel momentum representation of the three-dimensional surface problems can be easily written in terms of $\underline{G}_{E,\vec{k}_{||}}(z,z')$. If the probe process is sensitive only to one momentum component $\vec{k}_{||}$, this is the GF we need. If all the momentum components contribute to the probe process, we need to take the sum over $\vec{k}_{||}$ of $G_{E,\vec{k}_{||}}$. For example, Raman amplitudes can be written in the form

$$\int d\vec{k}_{||}\int dz\int dz'[\underline{\Psi}_f(z)]^{\dagger}\underline{X}(z)\underline{G}_{E,\vec{k}_{||}}(z,z')\underline{X}(z')\underline{\Psi}_i(z') ,$$

where $\underline{\Psi}_i$ and $\underline{\Psi}_f$ are for the initial and final states, X are the photon-matter matrix elements ($\langle\vec{k}''_{||}|X|\vec{k}'_{||}\rangle$) and the sum over $\vec{k}_{||}$ is over all possible parallel momentum vectors. If the initial state $|i\rangle$ has well-defined parallel momentum $\vec{k}_{\perp,i}$, then $\vec{k}_{||}$ equals the sum of $\vec{k}_{||,i}$ and the parallel component of momentum of the incident photon, so there is no need for the sum over $\vec{k}_{||}$.

We have demonstrated the utility and efficiency of the present GF approach for one-dimensional surface problems. Calculations with simple step-function model potentials as simple examples have been presented. The general trends observed for the surface DOS for an adatom on surface have been determined. If the isolated-adatom state lies within a band, its resonance width is large, whereas, if it lies within a band gap, the resonance state is quite narrow. Contribution to the surface DOS from the bulk DOS is skewed to higher energies. Surface states are pulled out of the bulk near the high-energy band edges. These trends were physically reasonable and predictable at the onset, but with the present GF method quantitative results are easy to obtain. This method can be used for

field-emission studies, low-energy electron-diffraction studies, etc. Detailed calculations in the three-dimensional case using this method have not been carried out as yet. It is of great interest to do so.

ACKNOWLEDGMENT

This work is supported in part by the U. S.-Israel Binational Science Foundation.

[1](a) F. Garcia-Moliner and J. Rubio, J. Phys. C 2, 1789 (1969); (b) F. Garcia-Moliner and J. Rubio, Proc. R. Soc. London Ser. A 324, 257 (1971).

[2]J. E. Inglesfield, J. Phys. C 4, L14 (1971).

[3]B. Velicky and I. Bartoš, J. Phys. C 4, L104 (1971).

[4](a) H. Ueba and S. G. Davison, J. Phys. C 13, 1175 (1980); (b) S. G. Davison, H. Ueba, and R. J. Jerrard, J. Phys. C 13, 1351 (1980); (c) R. J. Jerrard, H. Ueba, and S. G. Davison, Phys. Status Solidi B 103, 353 (1981).

[5]M. L. Glasser, Surf. Sci 64, 141 (1977).

[6]G. Oxinos and A. Modinos, Can. J. Phys. 58, 1126 (1980).

[7]R. Haydock, V. Heine, M. J. Kelly, and J. B. Pendry, Phys. Rev. Lett. 29, 868 (1972).

[8](a) D. Kalkstein and P. Soven, Surf. Sci. 26, 85 (1971); (b) G. Allan and P. Lenghart, *ibid.* 15, 101 (1969).

[9]S. K. Lyo and R. Gomer, *Interactions on Metal Surfaces,* Vol. 4 of *Topics in Applied Physics,* edited by R. Gomer (Springer, Berlin, 1975), p. 41.

[10]K. Kambe, Surf. Sci. 117, 443 (1982).

[11]Y. B. Band and B. M. Aizenbud, Chem. Phys. Lett. 77, 49 (1981); 79, 224 (1981); T. Lukes, in *Solid State Theory,* edited by P. T. Landsberg (Wiley, New York, 1969), Chap. XI, p. 407; R. G. Newton, *Scattering Theory of Waves and Particles* (McGraw-Hill, New York, 1966); J. R. Taylor, *Scattering Theory: The Quantum Theory of Nonrelativistic Collisions* (Wiley, New York, 1972).

[12]A. Messiah, *Quantum Mechanics* (Wiley, New York, 1968) Vol. I, p. 88.

[13]R. de L. Kronig and W. G. Penney, Proc. R. Soc. London Ser. A 130, 499 (1931).

[14]C. Kittle, *Introduction to Solid State Physics,* 5th ed. (Wiley, New York, 1976), p. 192.

[15]R. B. Gerger, L. H. Beard, and D. J. Kouri, J. Chem. Phys. 74, 4709 (1981).

[16]Y. B. Band, S. J. Singer, and K. F. Freed (unpublished).

[17]J. T. Hwang and H. Rabitz, J. Chem. Phys. 70, 4609 (1979).